Application of the x-Plot Technique to the Study of Water Influx in the Sidi El-Itayem Reservoir, Tunisia

I. Ershaghi, SPE, U. of Southern California
L.L. Handy, SPE, U. of Southern California
M. Hamdi, U. of Southern California

SPE 14209

Summary. The *x*-plot technique is extended and a relationship is developed between water throughput and water cut by use of field performance data. This relationship allows the estimation of water that has invaded the drainage area of a well, a group of wells, or a field under water injection or natural water influx. Applications to a simulated waterflood, an actual waterflood in Long Beach, CA, and the water influx in the Sidi El-Itayem reservoir in Tunisia are discussed.

Introduction

The *x*-plot technique introduced by Ershaghi and Omoregie[1] and Ershaghi and Abdassah[2] is a convenient method for representing oilfield performance history under water injection or natural water drive. The procedure is a linearization of water cut vs. recovery plot, allowing extrapolation to higher cuts. From the relationship

$$E_R = mx + n, \quad \ldots\ldots\ldots\ldots\ldots\ldots\ldots\ldots\ldots\ldots (1)$$

one may also derive a field composite relative-permeability-ratio curve.

Flood pot test data are often used to derive a relationship between water throughput and water cut. This approach requires the availability of core material representative of reservoir properties. Additionally, such core-derived correlations, which are based on laboratory relative-permeability curves, may not be extrapolated to actual field conditions because of layering and permeability variations that affect the field composite relative permeabilities.

Our experimentation with Eq. 1 in which both a reservoir simulation approach and actual field performance data were used shows that one may obtain a fair estimate of the cumulative water throughput at any high water cut from the slope of the *x*-plot.

This paper describes the proposed technique and its application to the Sidi El-Itayem reservoir in Tunisia, which is under a strong water drive.

Method Description

The *x*-plot procedure requires plotting $x = \ln(1/f_w - 1) - 1/f_w$ vs. fractional recovery. In the absence of layering effects and remedial profile corrections, a linear plot is obtained for cut values above 50%. The formation of a straight line indicates that the performance is being controlled by the relative-permeability-ratio characteristics of the reservoir.

If the oil recovery is expressed in terms of the fraction of oil in place (Eq. 1), then m and n may be used to obtain a field relative-permeability-ratio curve.

The amount of water throughput at any f_w from the frontal advance equation may be expressed as

$$V_{pi} = \frac{1}{(df_w/dS_w)}. \quad \ldots\ldots\ldots\ldots\ldots\ldots\ldots\ldots\ldots\ldots (2)$$

In practice, Eq. 2 requires a fieldwide relative-permeability-ratio curve. With a simple transformation of Eq. 1 and the derivation shown in Ref. 1 for df_w/dS_w, we have developed a procedure to obtain estimates of water throughput from the slope of the *x*-plot. If we express oil recovery in terms of actual volumes produced, Eq. 1 can be written as $x = m'N_p + n'$, where $m' = 1/(Nm)$ and $n' = -n/m$.

From Ref. 1,

$$V_{pi} = -1/[bf_w(1-f_w)] \quad \ldots\ldots\ldots\ldots\ldots\ldots\ldots\ldots\ldots\ldots (3)$$

and $b = 1/[m(1-S_{wi})]$. Therefore, with the definition for m',

$$V_{pi} = -m(1-S_{wi})/[f_w(1-f_w)]$$

$$= -(1-S_{wi})/[mNf_w(1-f_w)].$$

Now the water throughput in terms of actual volume can be estimated from

$$W_i = -B_{oi}/[m'f_w(1-f_w)], \quad \ldots\ldots\ldots\ldots\ldots\ldots\ldots\ldots (4)$$

where m' is in 1/vol.

Application to Waterflood

Application of Eq. 4 to both a simulated and an actual waterflood is demonstrated here. Fig. 1 shows the *x*-plot of Case 1, a simulated flood example discussed in Ref.

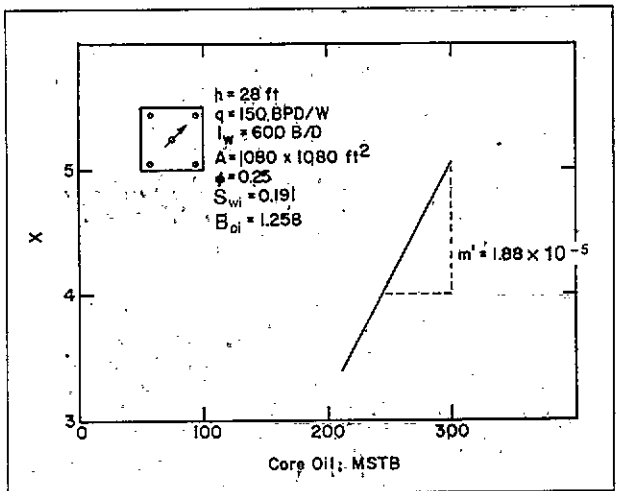

Fig. 1—x-plot of the simulated waterflood.

TABLE 1—PERFORMANCE OF THE SIMULATED WATERFLOOD

Year	Water Cut	x	Cumulative Oil (STB)
3	0.8881	3.1975	204,228
3.5	0.9066	3.3758	212,776
4	0.9200	3.5293	220,109
4.5	0.9295	3.6549	226,530
5	0.9369	3.7652	232,747
5.5	0.9429	3.8647	237,406
6	0.9478	3.9541	242,106
6.5	0.9520	4.0378	246,422
7	0.9556	4.1156	250,409
7.5	0.9586	4.1854	254,113
8	0.9614	4.2553	257,570
8.5	0.9637	4.3166	260,810
9	0.9657	4.372	263,864
10	0.9691	4.4775	269,506
12	0.9742	4.6577	279,288
15	0.9794	4.8877	291,259

$$W_i = \frac{1.258}{1.88 \times 10^{-5}(1-0.9794)(0.9794)} = 3{,}316{,}427 \text{ bbl}$$

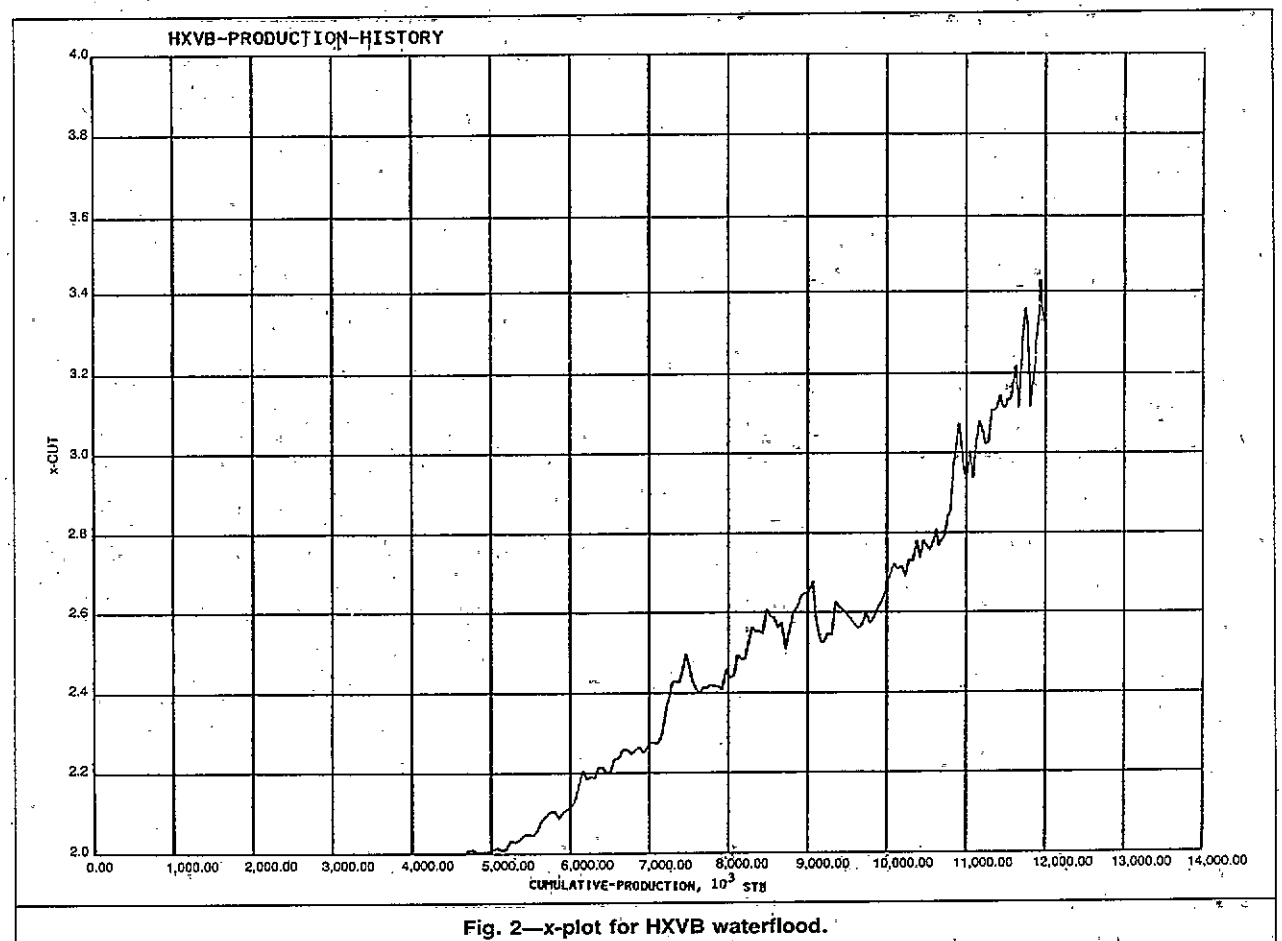

Fig. 2—x-plot for HXVB waterflood.

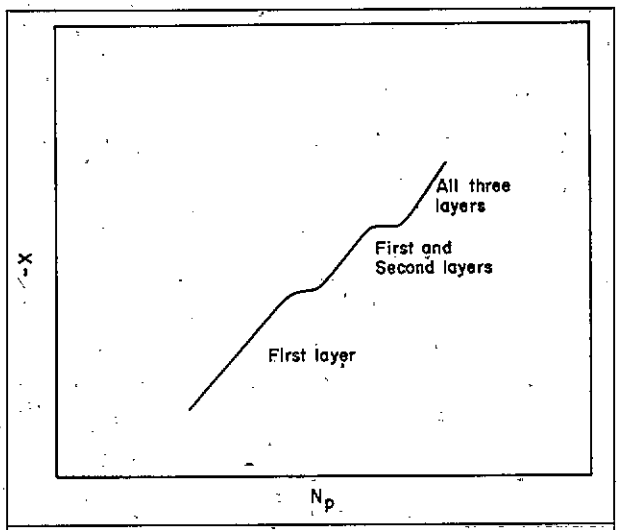

Fig. 3—x-plot for a hypothetical three-layer system.

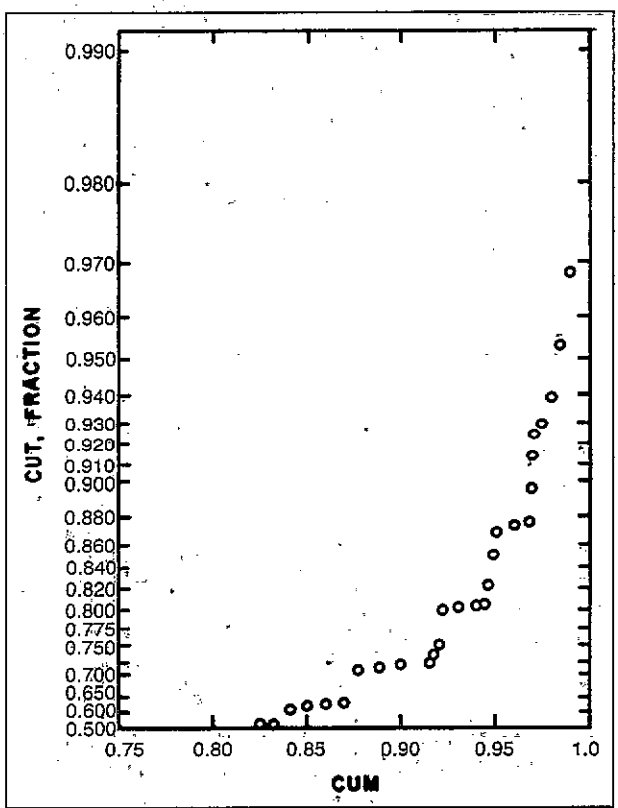

Fig. 4—x-plot for a 10-layer reservoir with mobility ratio = 0.125 (data from Snyder and Ramey[8]).

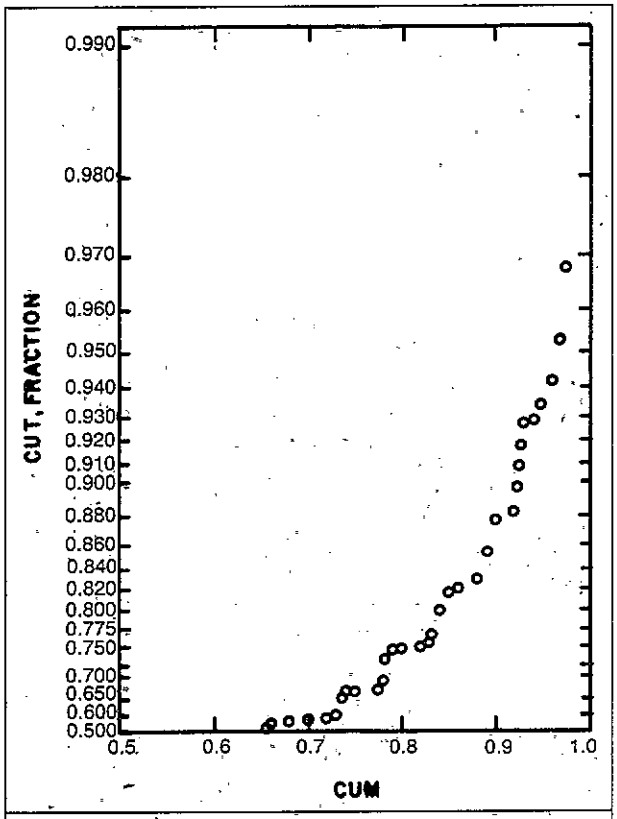

Fig. 5—x-plot for a 10-layer reservoir with mobility ratio = 1.0 (data from Snyder and Ramey[8]).

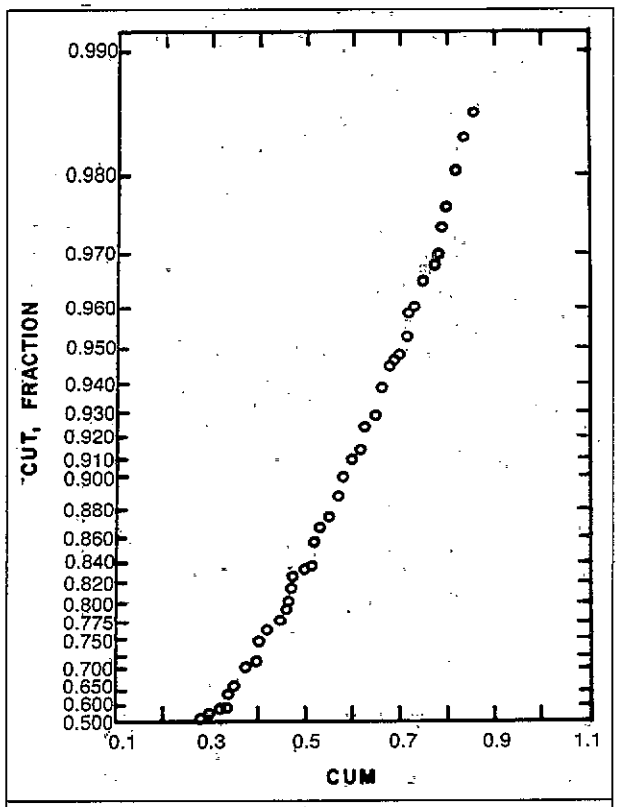

Fig. 6—x-plot for a 10-layer reservoir with mobility ratio = 10 (data from Snyder and Ramey[8]).

2. Table 1 shows the simulated performance data. The m' computed from the plot is 1.842×10^{-5} 1/bbl [11.6×10^{-5} 1/m^3]. At a water cut of 0.9794, this corresponds to a total injection of 3,316,427 bbl [527×10^3 m^3], verifying the actual injection of 3,285,000 bbl [522×10^3 m^3] (one injector at 600 BWPD [95 m^3/d water] for 15 years). Similar computations may be done for other simulated cases in Ref. 2.

Fig. 2 shows the x-plot for a waterflood in the HXVB sand in the Wilmington field, CA.* From the W_i calcula-

*Data are available from the California State Land Commission, Long Beach.

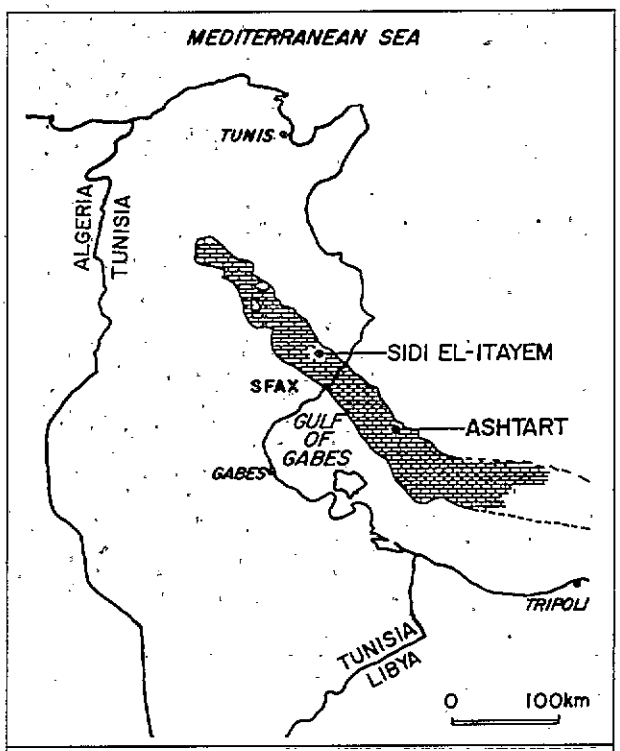

Fig. 7—Geographic location of the Sidi El-Itayem reservoir.

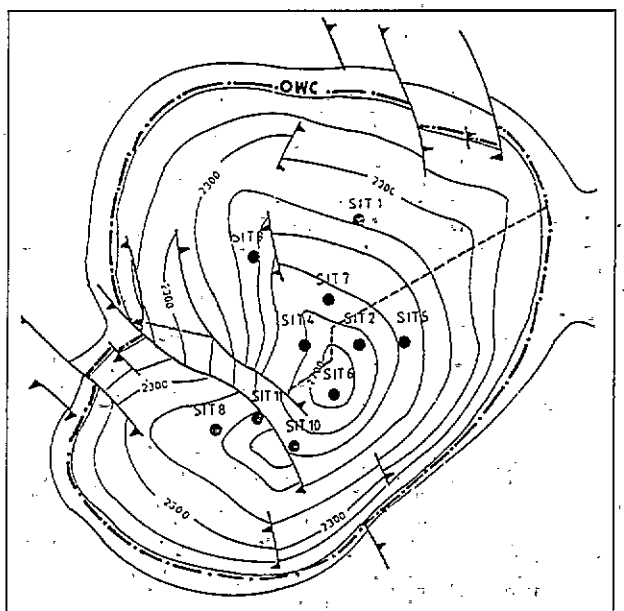

Fig. 8—Structural location of wells in Sidi El-Itayem.

TABLE 2—BASIC RESERVOIR ROCK AND FLUID PROPERTIES

Average formation thickness, ft	17
Original reservoir pressure, psi	3,385
Reservoir temperature, °F	246
Average porosity, %	8.4
Average matrix permeability, md	1.3
Average initial water saturation, %	0.2
Oil gravity, °API	40
Oil viscosity, cp	0.44
Water viscosity, cp	0.4
Bubblepoint pressure, psi	1,195
Initial oil FVF, RB/STB	1.24
Estimated initial oil in place, STB	132×10^6

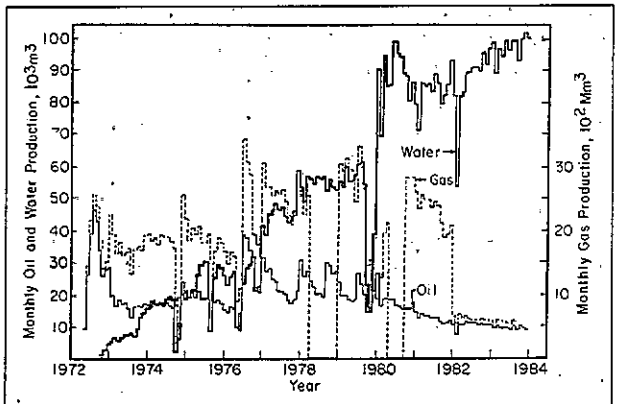

Fig. 9—Performance of the Sidi El-Itayem reservoir.

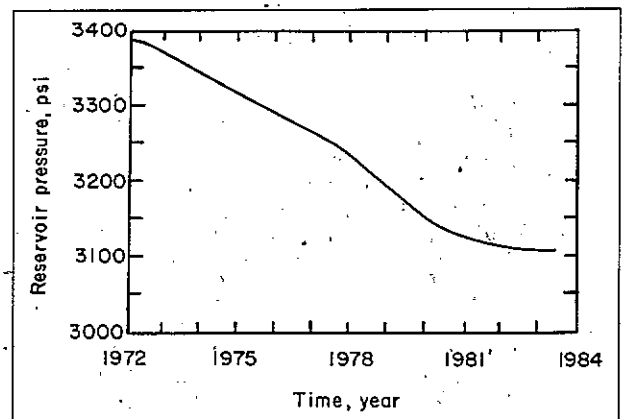

Fig. 10—Pressure history of the Sidi El-Itayem reservoir.

tion, the total influx at a cut of 0.9103 is estimated to be 76,530,431 bbl [12.2×10^6 m^3]. This is in excellent agreement with the actual injection volume of 77,516,746 bbl [12.3×10^6 m^3], considering the errors in the estimation of B_{oi} and m'.

Application to Water-Influx Calculations

Several techniques have been proposed to estimate cumulative water influx into oil and gas reservoirs. Among these are van Everdingen and Hurst's[3] unsteady-state theory, Fetkovitch's[4] approximate method, Carter and Tracy's method,[5] and the material-balance method.[6-8] Estimation of cumulative influx at any time with these techniques requires reservoir pressure data in addition to performance history.

The technique proposed here considers a water-drive reservoir to be analogous to a reservoir under water injection. Regardless of the injection rate and pressure, the cumulative water produced is controlled by the composite relative-permeability curve describing oil and water flow in the reservoir. The composite field relative-permeability ratio includes the influence of vertical sweep efficiency in the system.

TABLE 3—SUMMARY OF W_i COMPUTATIONS FOR SIDI EL-ITAYEM FIELD

x-plot	m' ($1/m^3$)	f_w (Dec. 1983)	W_i (10^6 m^3)	W_p (10^6 m^3)	N_p (10^6 m^3)	G_p (10^6 m^3)
Entire field	1.7×10^{-6}	0.9209	10.013	6.99	2.58	1.224
Southern part (Wells Sit-06, 08, 10 and 11)	6.47×10^{-6}	0.9467	3.79	3.35	0.843	0.433
Northern part (Wells Sit-01, 02, 04, 05, 07, and 09)	1.885×10^{-6}	0.8797	6.215	3.64	1.74	0.79
Well Sit-01	1.294×10^{-4}	0.8507	0.517	0.173	0.0907	0.028
Well Sit-02	1.294×10^{-4}	0.9410	1.726	1.987	0.978	0.533
Well Sit-04	2.022×10^{-4}	0.7106	0.240	0.054	0.189	0.056
Well Sit-05	2.647×10^{-5}	0.9471	0.934	0.844	0.224	0.106
Well Sit-06	2.647×10^{-5}	0.973	1.438	1.436	0.449	0.242
Well Sit-07	1.655×10^{-5}	0.8209	0.410	0.396	0.214	0.049
Well Sit-08	9.1×10^{-5}	0.9524	0.30	0.353	0.145	0.065
Well Sit-09	5.5×10^{-6}	0.8841	2.199	0.183	0.042	0.0169
Well Sit-10	4.101×10^{-5}	0.9515	0.654	0.49	0.10	0.054
Well Sit-11	2.891×10^{-5}	0.9641	1.239	1.076	0.149	0.071

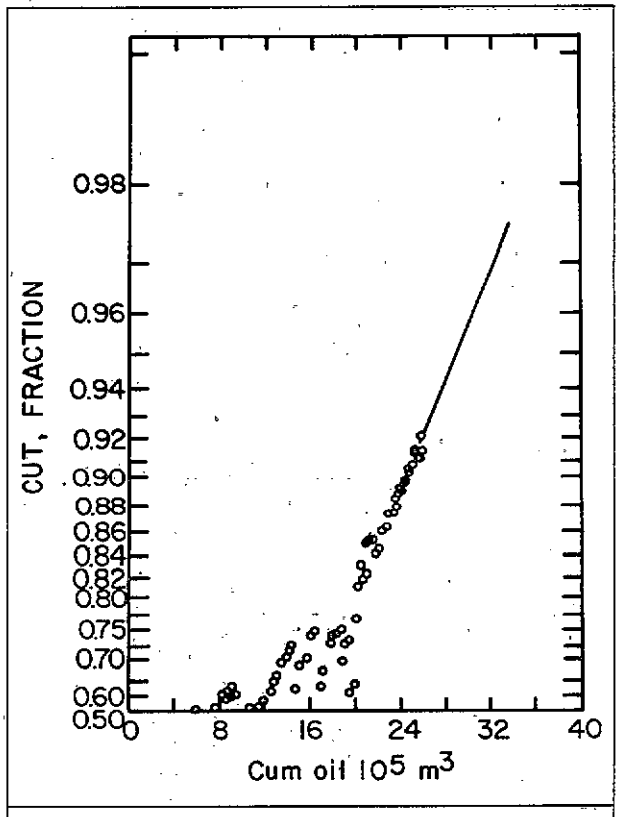

Fig. 11—x-plot of entire reservoir.

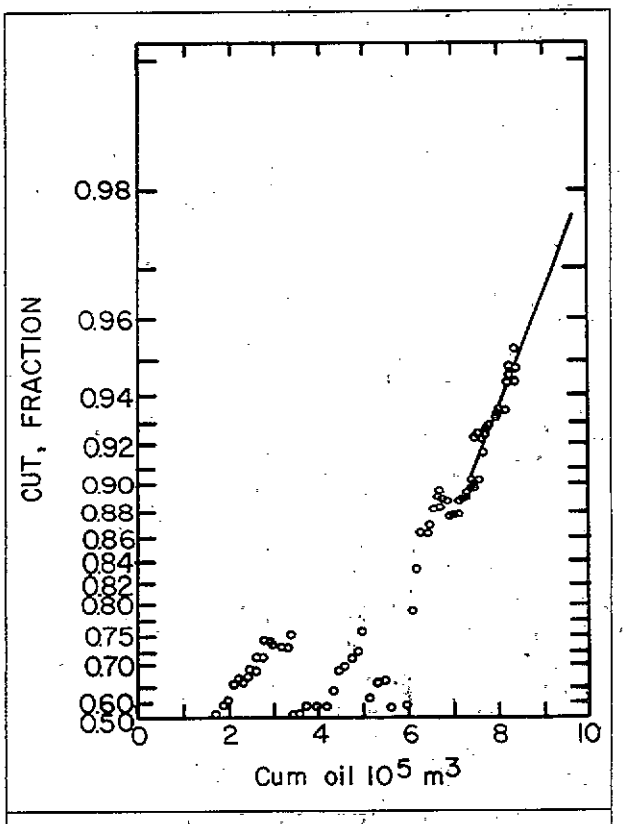

Fig. 12—x-plot of southern wells.

Consider an x-plot for a three-layer reservoir. As shown in Fig. 3, the breakthrough from successive layers results in a shifting of the plot. If the relative-permeability ratios characteristic of the three layers are identical, then the trends remain parallel. The final straight line represents the composite behavior of the reservoir. The slope of this composite trend is used to estimate the water influx at any high water cut.

As Snyder and Ramey[8] discussed for layered systems, the mobility ratio between water and oil also affects the shape of the curve of WOR vs. recovery. At mobility ratios of more than one, the step-function nature of the plot of x vs. recovery disappears and a smoother shape develops. Figs. 4 through 6 show the x-plot for mobility ratios of 0.125, 1, and 10, respectively. The curvature at the end of the plot is caused by the nature of the relative-permeability equations used by Snyder and Ramey.

Application to the Sidi El-Itayem Reservoir

The Sidi El-Itayem reservoir is located on the north side of Sfax, Tunisia (Fig. 7). This reservoir, discovered in July 1971, is a faulted carbonate reservoir consisting of several blocks (Fig. 8). The producing interval is nummulitic limestone consisting of three layers with a total thickness of 171 ft [52 m]. Core analysis data from three wells indicate low matrix permeabilities, ranging from 0.6 to 2.4 md, and porosities from 3.8 to 14.4%. Other details about reservoir properties are listed in Table 2.

TABLE 4—DATA FOR WATER INFLUX ESTIMATION FROM THE MATERIAL-BALANCE METHOD

N_p, STB	16.24×10^6
N, STB	132×10^6
B_{oi}, RB/STB	1.24
B_o, RB/STB	1.25
p_i, psia	3,185
p, psia	3,108
c_t, psi^{-1}	5×10^{-6}
S_{wi}	0.2
c_w	3.6×10^{-6}
W_p, bbl	43.9×10^6
c_o, vol/vol-psi	1.047×10^{-4}

$$W_e = N_p B_o + W_p B_w + \frac{NB_{oi}}{1-S_{wi}}(p_i - p)[c_o(1-S_{wi}) + c_f + c_w S_{wi}]$$

TABLE 5—RESERVOIR DATA FOR CALCULATION OF WATER INFLUX USING THE UNSTEADY-STATE APPROACH

c_t, psi^{-1}	8.6×10^{-6}
$\theta/360$	1
r_o, ft	6,100
B_w, RB/STB	1.00
U, bbl/psi	5,113
k, md	300
r_{eD}	10

$$W_e(t) = U \sum_{J=0}^{n-1} \Delta p_J W_D(t_D - t_{DJ})$$

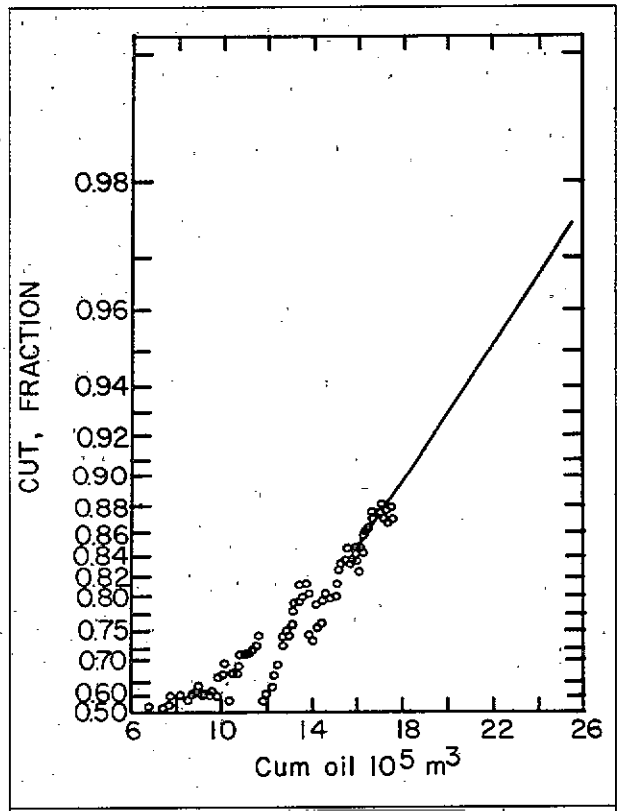

Fig. 13—x-plot of northern wells.

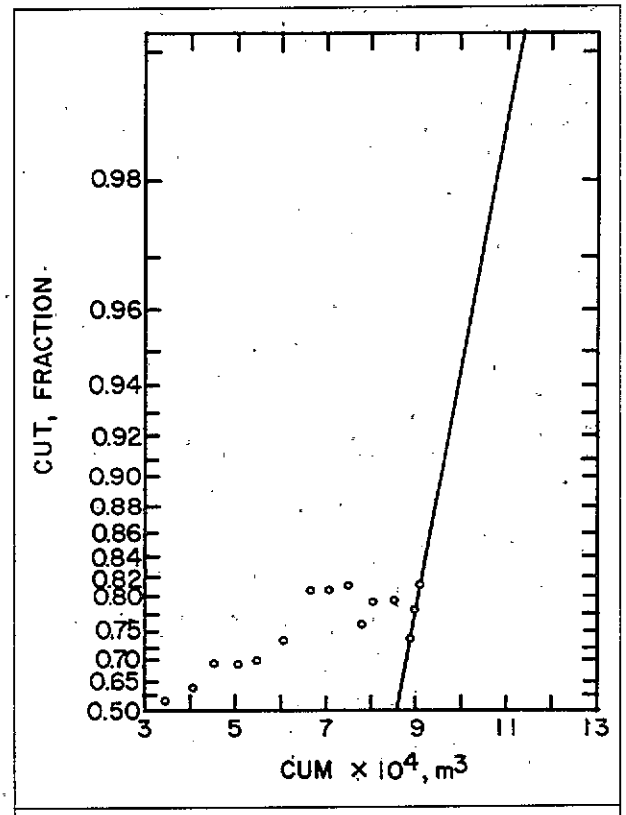

Fig. 14—x-plot of Well Sit-01.

The presence of an active aquifer in the field can be detected by examination of performance history. Increasing trends in WOR and a stabilization of reservoir pressure are shown in Figs. 9 and 10, respectively.

The rate of water cut increase vs. cumulative production in various wells shows a nonuniform pattern. Wells in the southern part of the reservoir have shown much greater increase rates than those in the north. Water production has been partially controlled through shutting down high-cut wells.

Table 3 shows a summary of the calculation of water influx volumes for the reservoir and individual wells estimated with the proposed procedure. Examination of the x-plot for the entire field (Fig. 11) shows an early trend relating to combined behavior of Wells Sit-01 through Sit-05. The addition of Well Sit-06 stabilized the cut, but a similar trend then developed and continued to the latter part of 1977. After that, the addition of Wells Sit-07 through Sit-11 resulted in a period of fluctuating cut. Well Sit-11 was completed in Oct. 1979, and a relatively stable trend developed with $m' = 0.27\times10^{-6}$ 1/bbl [1.70×10^{-6} 1/m^3]. This corresponds to an estimated water influx volume of 63×10^6 bbl [10.013×10^6 m^3] at a water cut of 0.9209 as shown below:

$$W_i = \frac{1.24}{1.7\times10^{-6}\times0.9209(1-0.9209)}$$

$$= 10.013\times10^6 \text{ m}^3.$$

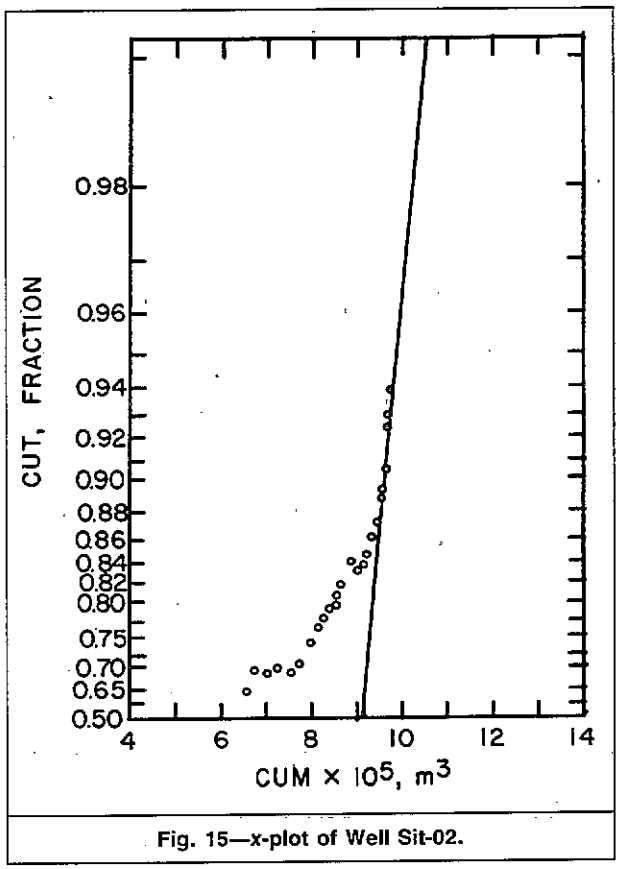

Fig. 15—x-plot of Well Sit-02.

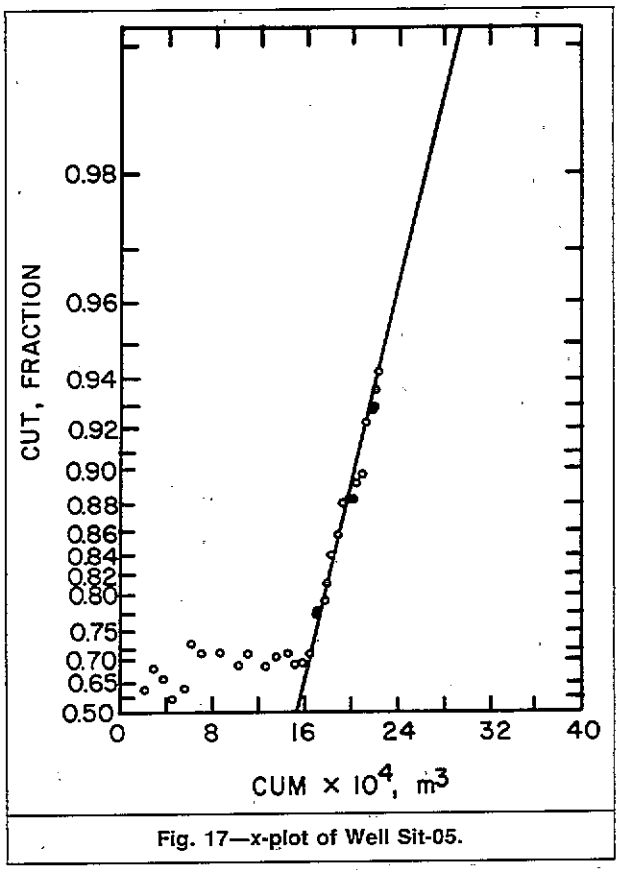

Fig. 17—x-plot of Well Sit-05.

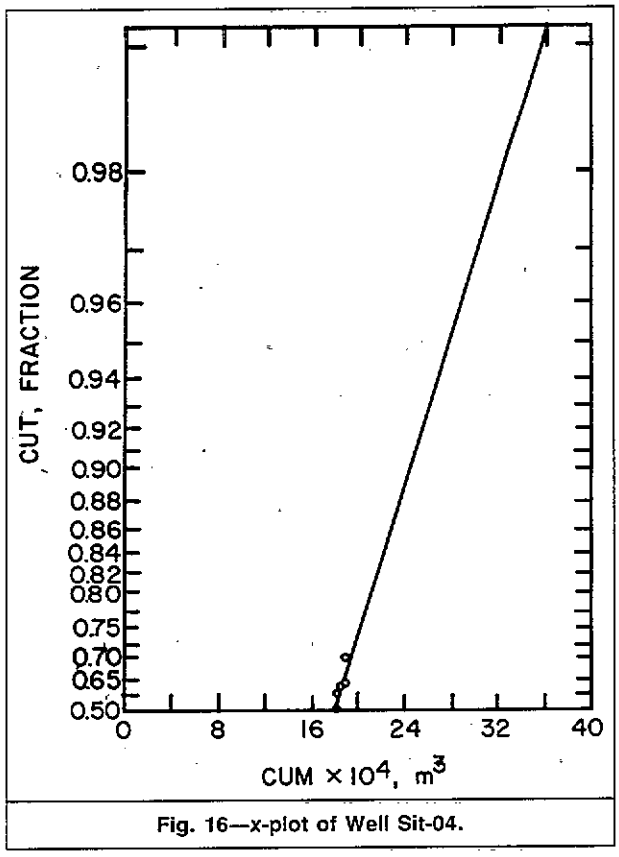

Fig. 16—x-plot of Well Sit-04.

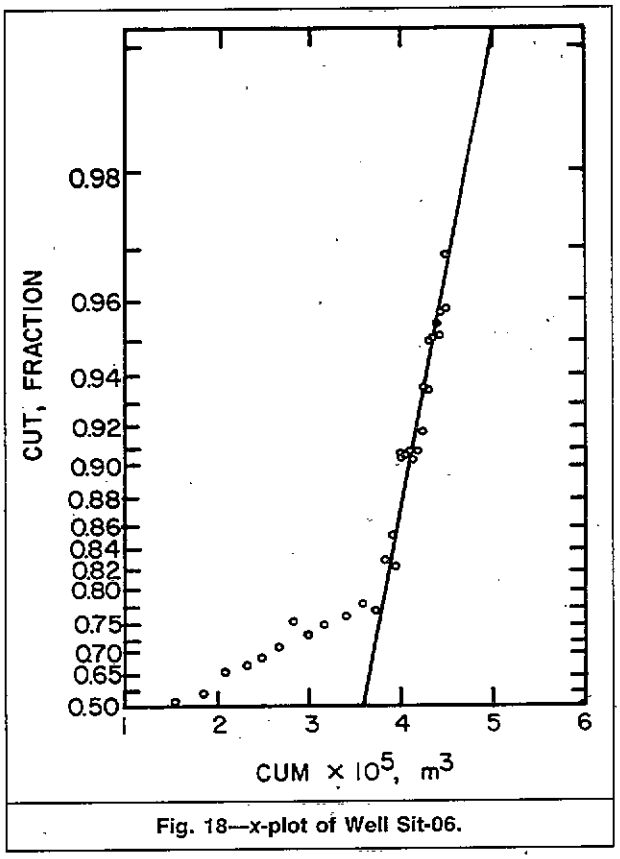

Fig. 18—x-plot of Well Sit-06.

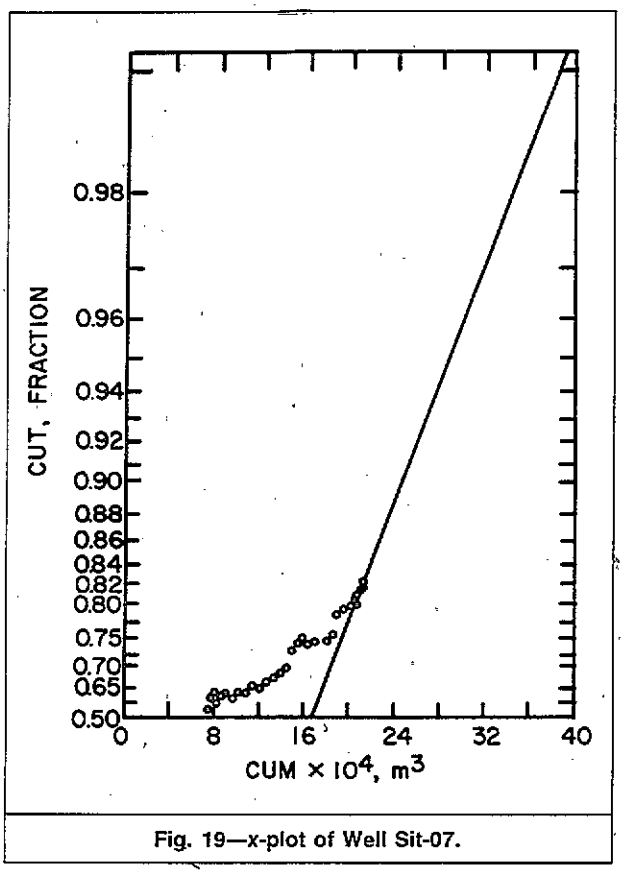

Fig. 19—x-plot of Well Sit-07.

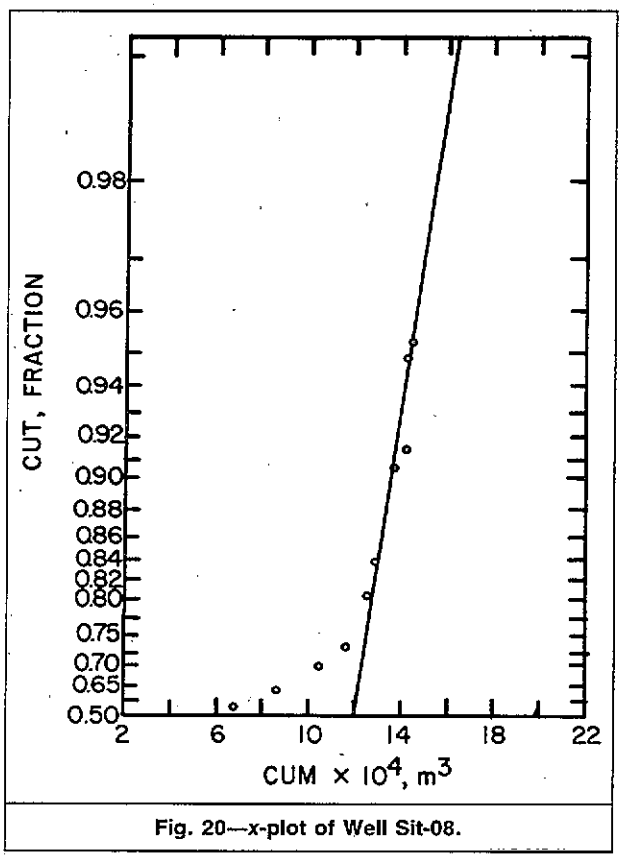

Fig. 20—x-plot of Well Sit-08.

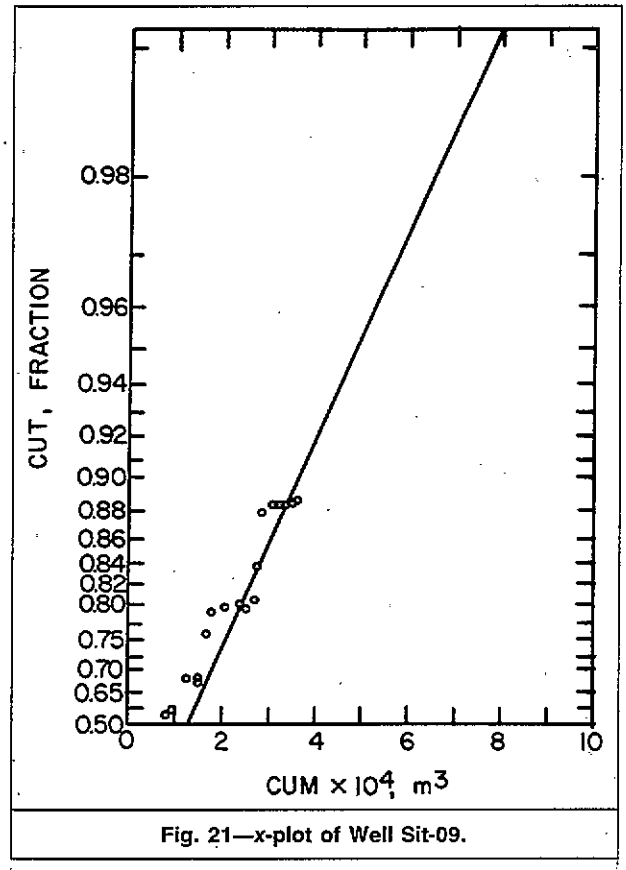

Fig. 21—x-plot of Well Sit-09.

From a material-balance calculation for this reservoir, which is above the bubblepoint, we obtained an influx of 65×10^6 bbl [10.399×10^6 m^3]. Basic data used in the material-balance calculation are shown in Table 4.

We also used the unsteady-state equation of the van Everdingen and Hurst[3] method to verify the results. Table 5 shows the additional information used for this approach. If one uses a matrix permeability of 1 to 2 md, very unreasonable answers are obtained at any acceptable range of r_{eD}. By a trial-and-error procedure, we noticed that, for example, use of k=200 md and r_{eD}=10 results in W_i=63×10^6 bbl [10.07×10^6 m^3]. This permeability is much larger than the matrix permeability, which indicates the presence of a high-permeability fracture network in the reservoir.

Analysis of W_i Calculations

The ability to estimate water influx into the drainage area of individual wells opens up new possibilities for reservoir characterization. For example, the directional trend of water movement can be mapped and the performance of wells can be compared at similar positions with respect to the water/oil contact. If the slopes of the x-plots for individual wells were equivalent, then the chronological contours of the W_i's would have the same features as the contours of the equivalent water cuts. But when wells exhibit different slopes, at a given water cut the W_i's for individual wells would be different. This is an important diagnostic tool for estimating reservoir heterogeneities.

For the Sidi El-Itayem field, we computed a total of 23.8×10^6-bbl [3.79×10^6-m^3] influx from the south, using the combined performance of Wells Sit-06, 08, 10, and 11 shown in Fig. 11. In a separate calculation, we

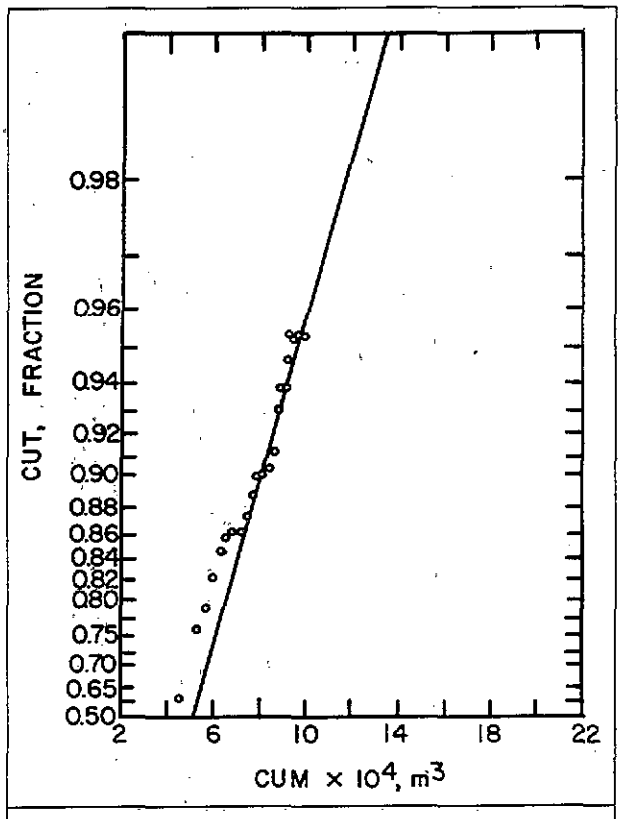

Fig. 22—x-plot of Well Sit-10.

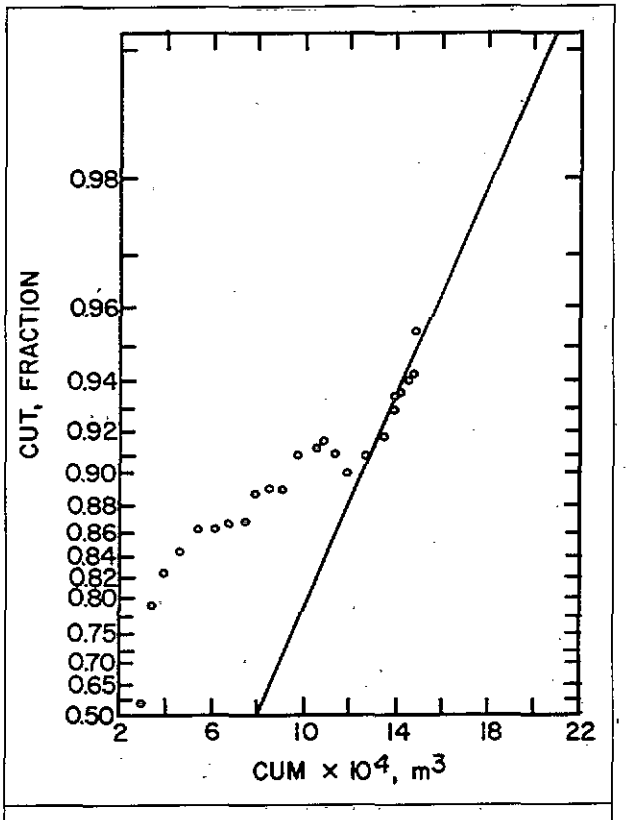

Fig. 23—x-plot of Well Sit-11.

obtained 39×10^6 bbl [6.215×10^6 m^3] of influx from the northern wells (Sit-01, 02, 04, 05, 07, and 09) shown in Fig. 12. The sum of the two agrees reasonably well with the influx computed for the entire reservoir. The slope of the combined performance of the southern wells indicates poorer recoveries than for the wells in the northern part.

Similarly, the x-plot slope for individual wells and groups of wells may be compared (Figs. 11 through 23). Among the southern wells, for example, Well Sit-08 with the largest slope shows a lower W_i than Well Sit-10 at a similar water cut. This means that if Well Sit-08 had continued producing, one would have expected a water cut of 0.98 by the time 4×10^6 bbl [0.654×10^6 m^3] of water had invaded its drainage area. Well Sit-10 showed a cut of only 0.9515 for this amount of invasion.

Conclusions

1. As an extension of the x-plot technique, a method is proposed that allows estimation of water throughput at any water cut by the use of field performance data.
2. Application of the procedure has been demonstrated for waterflood and water-influx calculations.
3. Comparison of W_i's computed for individual wells in a given field can serve as a measure of directional movement of water and reservoir heterogeneities.

Nomenclature

b = slope of k_o/k_w vs. S_w on semilog paper
B = FVF, RB/STB [res m^3/stock-tank m^3]
c = compressibility, vol/vol-psi [vol/vol·kPa]
E_R = overall reservoir recovery efficiency, N_p/N, bbl [m^3]
f_w = fractional water cut
G_p = cumulative gas produced, scf [std m^3]
h = thickness, ft [m]
k = permeability, md
m = slope in Eq. 1, dimensionless
m' = slope of x vs. N_p, 1/vol
n = intercept in Eq. 1, dimensionless
n' = intercept in plot of x vs. N_p, dimensionless
N = initial oil in place, STB [stock-tank m^3]
N_p = cumulative oil production, bbl [m^3]
p = pressure, psi [kPa]
q = flow rate, B/D [m^3/d]
r = radius, ft [m]
r_{eD} = r_e/r_o, dimensionless aquifer ratio
S = saturation, fraction
t = time, years
t_D = dimensionless time
U = $2\pi\phi hcr_o{}^2\theta/360$, aquifer constant
V_{pi} = number of PV's invaded
W_e = estimated volume of water influx, bbl [m^3]
W_i = actual volume of water invaded, bbl [m^3]
W_p = cumulative water produced, bbl [m^3]
x = $\ln(1/f_w-1)-1/f_w$
μ = viscosity, cp [Pa·s]
ϕ = porosity, fraction
θ = encroachment angle, degrees [rad]

Subscripts

D = dimensionless
e = external
f = fracture

i = initial
o = oil
t = total
w = water

Acknowledgments

Data on Sidi El-Itayem f eld were furnished by ETAP in Tunisia. We thank Habil Lazerg and Mongi Azzouz for their support during the course of this study. We also thank Marsha Ershaghi, Saba Tahmassebi, Katherine Barnes, and Tony Lam for their assistance during the preparation of this paper.

References

1. Ershaghi, I. and Omoregie, O.: "A Method for Extrapolation of Cut vs. Recovery Plots," *JPT* (Feb. 1978) 203-04.
2. Ershaghi, I. and Abdassah, D.: "A Prediction Technique for Immiscible Processes Using Field Performance Data," *JPT* (April 1984) 664-70.
3. van Everdingen, A.F. and Hurst, W.: "Application of the Laplace Transformation to Flow Problems in Reservoirs," *Trans.*, AIME (1949) 305-24.
4. Fetkovich, M.J.: "A Simplified Approach to Water Influx Calculations—Finite Aquifer Systems," *JPT* (July 1971) 814-28.
5. Carter, R.D. and Tracy, G.W.: "An Improved Method for Calculating Water Influx," *JPT* (Dec. 1960) 58-62; *Trans.*, AIME, **219**.
6. Havlena, D. and Odeh, A.S.: "The Material Balance as an Equation of a Straight Line," *JPT* (Aug. 1963) 896-900; *Trans.*, AIME, **228**.
7. van Everdingen, A.F., Timmerman, E.H., and McMahon, J.J.: "Application of the Material Balance Equation to a Partial Water-Drive Reservoir," *JPT* (Feb. 1953) 51-58; *Trans.*, AIME, **198**.
8. Snyder, R.W. and Ramey, H.J. Jr.: "Application of Buckley-Leverett Displacement Theory to Noncommunicating Layered Systems," *JPT* (Nov. 1967) 1500-05; *Trans.*, AIME, **240**.

SI Metric Conversion Factors

°API	141.5/(131.5+°API)		=	g/cm^3
bbl	× 1.589 873	E−01	=	m^3
cp	× 1.0*	E−03	=	Pa·s
ft	× 3.048*	E−01	=	m
ft^2	× 9.290 304*	E−02	=	m^2
°F	(°F−32)/1.8		=	°C
in.	× 2.54*	E+00	=	cm
mile	× 1.609 344*	E+00	=	km
psi	× 6.894 757	E+00	=	kPa
psi^{-1}	× 1.450 377	E−01	=	kPa^{-1}

*Conversion factor is exact.

JPT

Original manuscript received in the Society of Petroleum Engineers office Sept. 22, 1985. Paper accepted for publication April 15, 1987. Revised manuscript received June 2, 1987. Paper (SPE 14209) first presented at the 1985 SPE Annual Technical Conference and Exhibition held in Las Vegas, Sept. 22-25.